International Journal of Mechatronics and Applied Mechanics
2025, Issue 22, Vol. I

EFFECTS OF SOIL PROPERTIES AND CRATERING FROM MINE DETONATION ON SHOCK WAVE PROPAGATION AND THE DYNAMIC RESPONSE OF REMOTE DEMINING VEHICLE STRUCTURES

Denys Tkachenko[1][0000-0002-5006-6775], Vadym Garin[2][0000-0001-7788-0593], Vitalii Myntiuk[2][0000-0002-4047-0192] , Olga Shypul[2][0000-0002-1356-5831], Oleksiy Pavlenko[2][0000-0002-1628-2239]
[1]Department of Aircraft Strength, National Aerospace University "Kharkiv Aviation Institute", Vadym Manka str. 17, 61070, Kharkiv, Ukraine
[2]Department of Aircraft Production Technology, National Aerospace University "Kharkiv Aviation Institute", Vadym Manka str. 17, 61070, Kharkiv, Ukraine
Email: v.garin@khai.edu

Abstract - This paper investigates methods for accurate soil modelling and evaluates the effect of including soil in computational models on predicting the stress-strain response of a gas-detonation deminer located near the epicentre of a mine explosion. The study assesses the structural behaviour under the influence of direct and reflected shock waves generated by detonations on different soil types. Among existing approaches for numerically modelling explosive processes and shock-wave effects on nearby structures, the ALE method implemented in the LS-DYNA software package was selected. In cases where soil was included in the model as an independent physical domain, four types of sandy soils were considered: unwashed sand, low-density dry sand, high-density sand with natural moisture, and high-density water-saturated sand. Validation of the computational model demonstrated convergence of key characteristics: the kinetic energy acquired by the deminer from the blast impact, displacements of the flange of the most compliant pipe, and the geometry of the crater in the soil. Results show that reflected blast waves from the soil surface contribute energy levels to the structure comparable to those from the primary detonation, significantly influencing internal energy accumulation and structural deformation. Neglecting realistic soil properties or replacing the soil domain with simplified boundary conditions can lead to 25–45% errors in predicting the stress-strain response. The proposed model enables accurate simulation of crater geometry, soil ejection, and blast-structure interaction, providing a validated basis for optimizing gas-detonation deminer design under diverse geotechnical conditions.

Keywords: Gas detonation deminer; Explosive processes; Direct and reflected shock waves; Soil modelling.

1. Introduction

Since the beginning of the full-scale invasion, Ukraine has faced widespread contamination of land with mines and unexploded ordnance. To date, more than 150,000 km^2 of territory requires demining.

Modern demining strategies focus on keeping personnel at a safe distance from dangerous areas while minimizing direct contact with explosive devices. Consequently, technologies that allow deminers to avoid being physically present at detonation sites are becoming increasingly important. These technologies include unmanned ground vehicles, aerial platforms, and remotely operated mobile platforms equipped with both contact tools (such as cutters) and noncontact tools (like explosives) for mine neutralization.

Contact demining vehicles approach mines directly, disturb the ground, or remove the upper soil layers to trigger detonation through mechanical interaction. However, these systems are exposed to risks from shockwaves and shrapnel, often experience malfunctions, and require reinforced protection for their hulls and suspensions.

In contrast to traditional methods, noncontact demining vehicles initiate detonation from a safe

https://doi.org/10.17683/ijomam/issue22.v1.22

distance using low power pulse charges spaced at intervals or firing systems with directed cumulative charges and detonating gas mixtures. This approach protects the main structure of the vehicle from direct exposure to the shockwave or seismic impulse, as the explosion occurs outside the vehicle. As a result, there is a reduced risk of damage to the vehicle's mechanisms and electronic components. These technologies enhance operator safety, decrease maintenance costs, and improve demining efficiency.

A prototype of a gas-detonation based deminer has been proposed [1], operates on the principle of directed gas detonation jets that can initiate mine explosions from a safe distance. While this solution has shown effectiveness, its performance is highly dependent on the properties of the medium into which the detonation jet is directed. In real-world scenarios, the device must function effectively across diverse natural and anthropogenic environments. The characteristics of the upper soil layer significantly impact shockwave propagation, impulse reflection, and the dynamic response of the vehicle structure.

This is particularly relevant in Ukraine, where mine contaminated lands vary greatly in geological composition from loose sands in the south to dense chernozems in central regions and compacted clay or asphalt in urban areas. Variations in soil density, moisture, porosity, and cohesion influence how the gas detonation jet propagates and how explosion products disperse through both the air and the soil column.

This study aims to evaluate and justify the selection of suitable computational ground models for accurately simulating shockwave propagation and crater formation resulting from mine detonation. It also includes an analysis of the dynamic response of a noncontact deminer structure. Specifically, the research focuses on the following objectives:

- Examining how sensitive the results are to the level of discretization in the computational domain.
- Determining the optimal dimensions for the computational model.
- Analysing the dynamic response of the structure under various soil models and different physical and mechanical properties of the ground.

2. Current Approaches to Numerical Modelling

Modelling mine detonation and assessing its impact on structures is one of the most challenging tasks in the numerical analysis of dynamic processes. The complexity of this task arises from the interaction of multiple physical media – explosives, air, soil, and structural materials – under extreme conditions characterized by nonstationarity and high-pressure gradients. Each of these media has fundamentally different mechanical properties, which necessitate specific numerical treatments. Within the LSDYNA software suite [2] and similar environments, various methodological strategies [3 – 5] have been developed to model key components such as mines, soil, air, and structural systems.

One of the most widely used methods is the Arbitrary Lagrangian-Eulerian (ALE) approach [6 – 9]. In this scheme, the air, detonation products, and sometimes the soil are treated as Eulerian media, while the structure is modelled using Lagrangian bodies. This hybrid configuration effectively simulates shock wave-structure interactions using coupling algorithms like CONSTRAINED_LAGRANGE_IN_SOLID and ALE_COUPLING_NODAL_PENALTY. The primary advantage of the ALE method is its robustness in describing detonation wave propagation and its interaction with solids across a broad pressure range. However, this method is computationally intensive, particularly in three-dimensional simulations, and it presents challenges in maintaining stability and preventing material flow across phase boundaries.

The Smoothed Particle Hydrodynamics (SPH) method [5, 8, 10] is gaining popularity as an alternative to the ALE approach. SPH is especially effective for modelling soil behaviour near explosive charges, where large deformations, fractures, and mass redistribution occur. These phenomena are often difficult to capture with mesh-based methods. Additionally, SPH avoids mesh distortion and element degeneration, which are critical limitations when modelling soil ejection. However, SPH has some drawbacks. It is highly sensitive to discretization parameters and usually requires a much larger number of particles to achieve accuracy comparable to ALE, especially in heterogeneous media. Another one is the instability in representing boundary conditions at the interfaces between SPH domains and Lagrangian bodies, which can lead to uncontrolled particle penetration. This issue necessitates specialized coupling algorithms to maintain physical accuracy.

To overcome the limitations of individual methods, hybrid approaches have been developed. The most established hybrid combines ALE for modelling air and detonation products with SPH for the soil. This combination provides a more realistic representation of the granular nature of soil in the vicinity of the charge while retaining ALE's advantages in simulating wave propagation and interactions with structural elements. However, careful calibration is required to ensure accurate coupling, particularly during the transition of the blast wave from ALE-modelled air to SPH-modelled soil.

Despite these challenges, the ALE–SPH hybrid approach is promising, especially for simulations involving soil ejection and its subsequent impact on structures.

Some studies have also explored the use of the Discrete Element Method (DEM) for soil modelling [3]. DEM represents soil as a system of interacting solid particles connected by elastic bonds, enabling high-fidelity modelling of effects such as segregation, frictional interaction, and decompaction during explosive events. However, its wider application is limited by the difficulty of directly correlating DEM parameters with laboratory soil data, which restricts its use in practical engineering simulations.

Considering the specific requirements for modelling the effects of gas-detonation jets on explosive devices on the ground surface, the most suitable numerical strategy is to apply the ALE method for the air, detonation products, and soil, in combination with the Lagrangian formulation for the structure. This approach enables accurate and consistent simulation of detonation wave dynamics, their reflection, and interaction with the demining platform. The ALE model provides a comprehensive representation of all key aspects of the scenario from wave generation in the gas mixture to its propagation through the inhomogeneous soil and its interaction with the structure. Accurate modelling of the "mine-soil-air-structure" system is crucial, as the nature of this interaction determines the magnitude of impulse loads experienced by the deminer. This, in turn, directly impacts the durability and operational effectiveness of the system.

3. Mathematical Model and Problem Statement

To quantitatively analyse the impact of an explosion on the structure of a non-contact gas-detonation deminer, we developed a three-dimensional finite element model. The model captures the key physical media involved in the process: explosive, air, soil, and the structural components of the demining device (Figure 1). The formulation was designed to simulate not only the direct action of the blast wave but also secondary effects, such as shock wave reflection from the ground surface and its interaction with structural elements.

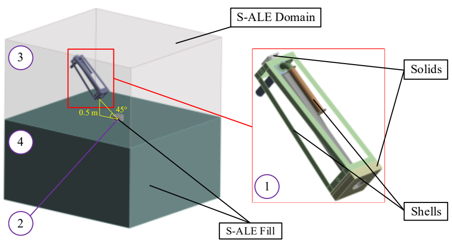

Figure 1. Structure of the computational model: 1. deminer (see [1]); 2. mine; 3. air; 4. ground

A hybrid Multi-Material Arbitrary Lagrangian–Eulerian (MMALE, or simply ALE) approach was applied to describe the continua involved in the explosion [3, 5]. All continuous media (air, soil, and detonation gases) were modelled using a specialized Eulerian multi-material mesh with the ELFORM = 11 formulation [11], which allows multiple materials to coexist within a single element. This approach ensures accurate reproduction of interfacial dynamics, including shock wave propagation, material flow, and detachment zones. Each material within the MMALE domain was assigned to a separate group, allowing for precise specification of physical and mechanical properties, as well as interaction parameters with the structure.

The structure of the gas-detonation deminer was modelled using a Lagrangian formulation, incorporating both shell and solid finite elements. The protective plates, mixing chamber, and central connector were modelled using solid elements with the Fully Integrated S/R Solid formulation [11], which provides high accuracy in representing the stress-strain state under impulsive loading. Simpler structural components like pipelines, flanges, and frame elements of the protective casing were represented using shell elements with the Belytschko-Tsay formulation [11]. This formulation is commonly used in short-duration dynamic simulations due to its computational efficiency. To ensure adequate accuracy in stress distribution across the cross-section, five through-thickness integration points were assigned to the shell elements.

The interaction between the Eulerian media and Lagrangian structural bodies was conducted using the CONSTRAINED_LAGRANGE_IN_SOLID contact algorithm [3, 5, 11], which ensures proper coupling in fluid-structure interaction problems. A standard penalty-based coupling scheme was applied for both shell and solid elements. This scheme incorporates the surface normals of the structural components, ensuring physically accurate momentum transfer and prevents unintended interactions in potential detachment zones. Each element on the Lagrangian surface was assigned three coupling points (NQUAD = 3), providing an optimal balance between interface accuracy and numerical stability. Additionally, the LEAKAGE_CONTROL = STRONG option was activated to ensure proper handling of sharp pressure gradients at the interfaces between air, detonation products, and solid structures.

3.1 Modelling the Deminer's Design

Accurately simulating explosive loading requires selecting an appropriate material model to describe the behaviour of metal structures undergoing high-rate plastic deformation.

As demonstrated in [12], the most reliable representation of steel strength characteristics during blast loading is achieved using the MAT_POWER_LAW_PLASTICITY model (MAT_018 in the LS-DYNA material library) [13]. This is an isotropic elastic-plastic model with power-law hardening that accounts for strain-rate effects by modifying stresses according to the Cowper-Symonds yield model.

The material yield stress, σ_y in this model is described by the equation:

$$\sigma_y = k(\varepsilon_{yp} + \bar{\varepsilon}^{pl})^n, \quad (1)$$

where ε_{yp} is the elastic strain to yield, $\bar{\varepsilon}^{pl}$ is the effective (logarithmic) plastic strain, and *k* and *n* are power-law constants.

The strain-rate effect is incorporated using the Cowper-Symonds model, which scales the stresses in the plastic zone with the dynamic increase factor (DIF):

$$DIF = 1 + \left(\frac{\dot{\varepsilon}}{C}\right)^{1/q}, \quad (2)$$

where C and q are user-defined strain-rate sensitivity parameters, and $\dot{\varepsilon}$ is the current strain rate.

In this study, two steel grades were used: structural steel (for the hull and load-bearing elements) and rolled homogeneous armour (RHA) steel (for the protective plate). Their mechanical properties, including elastic modulus, yield strength, and hardening parameters, are summarized in Table 1. The values for the hardening constants and strain-rate sensitivity parameters were selected based on available literature [14].

Table 1. Steels mechanical properties

Property	Density, kg/m^3	Young`s modulus, GPa	Poisson`s ratio	Yield stress, MPa	*k*, MPa	*n*	*C*	*q*
RHA	7850	210	0.28	950	1560	0.0918	3200	5
Structural Steel	7850	210	0.28	250	557	0.119	40.4	5

3.2 Modelling the Detonation of an Explosive Charge (Mine)

To describe the thermodynamic properties of explosive detonation products in numerical simulations, the Jones-Wilkins-Lee (JWL) equation of state is used [13, 15]. This equation is widely employed in LS-DYNA to calculate the impulse effects of explosions. It defines the relationship between pressure (*p*), relative volume (υ), internal energy per unit volume (E_1) and has the form:

$$p = A\left(1 - \frac{\omega}{R_1\upsilon}\right)\exp(-R_1\upsilon) + B\left(1 - \frac{\omega}{R_2\upsilon}\right)\exp(-R_2\upsilon) + \frac{\omega E_1}{\upsilon}, \quad (3)$$

where A, B, R_1, R_2, and ω are material constants that characterize the behaviour of detonation products across a wide pressure range from peak conditions to hydrodynamic equilibrium.

The JWL equation is used in combination with the MAT_HIGH_EXPLOSIVE_BURN material model, which simulates the ignition and propagation of the detonation front. In this framework, the material model governs the combustion dynamics, while the equation of state determines the pressure at each time step after initiation. The MAT_HIGH_EXPLOSIVE_BURN model (Material Type 8) implements combustion based on the classical Wilkins model [16], where each element is ignited at a time calculated from its distance to the detonation point and the specified detonation velocity. From this ignition time, a combustion coefficient is derived, which scales the pressure values computed via the JWL equation. In this study, the model is used with the setting BETA = 0, which enables a combination of programmed burn and automatic (volume-dependent) combustion normalized to the Chapman-Jouguet (CJ) state. In this mode, the combustion coefficient is computed as a function of both time from initiation and the element's compression relative to the critical volume VCJ, which corresponds to the CJ state. This allows for the simulation of natural reaction propagation in the explosive medium without explicitly modelling the geometry of the detonation front.

Trinitrotoluene (TNT) was selected as the explosive material, representing a standard high explosive. Its physical properties are summarized in Table 2, and the JWL equation parameters are listed in Table 3.

Table 2. High Explosives properties for TNT

Density, kg/m^3	Chapman-Jouguet pressure, GPa	Detonation velocity, m/s	BETA
1630	21	6930	0.0

Table 3. The parameters of JWL Equation of state

A, GPa	*B*, GPa	R_1	R_2	ω	E_1, GPa
371.2	3.231	4.15	0.95	0.3	7

The geometry of the explosive charge significantly influences shock wave characteristics, particularly in the near field. As noted in [17], charge shape plays a crucial role within the scaled distance range:

$$Z = \frac{R}{\sqrt[3]{M}}, \quad (4)$$

where R is the actual distance from the charge and M is the explosive mass in TNT equivalent. The most significant variations in pressure distribution occur at scaled distances $Z < 1\ m/\sqrt[3]{kg}$.

Since most structural components of the gas-detonation deminer fall within this critical zone, the charge geometry was explicitly accounted for in the model. The mine was represented as a cylindrical charge with a diameter of 250 mm and a height of 100 mm scaled down proportionally from the TM-62T anti-tank mine (320 mm × 128 mm) to yield an equivalent explosive mass of 7.86 kg at a density of 1630 kg/m^3 (see Table 2).

Modelling of post-detonation combustion effects (the AFTERBURN option) was not included in this study. This decision is justified by the fact that, in open-field detonation scenarios, the thermal contribution of post-combustion is negligible compared to the internal thermal loads resulting from the detonation of the gas-air mixture within the device.

3.3 Air Modelling

To describe the air medium in explosive impact problems, we use an ideal gas model based on the gamma law. This model relates pressure to density and specific internal energy. It's considered appropriate for short-duration, high-intensity shock phenomena like blast wave propagation, especially in the near-field region close to the explosion's epicentre.

In LS-DYNA, this physical model is implemented using two keyword cards [5, 12, 13]:

*MAT_NULL: This defines the basic physical properties of air, such as initial density and viscosity;

*EOS_LINEAR_POLYNOMIAL: This specifies the equation of state by expressing pressure as a polynomial function of relative compression and internal energy per unit volume.

The equation of state has the following general form:

$$p = C_0 + C_1 m + C_2 m^2 + C_3 m^3 + (C_4 + C_5 m + C_6 m^2) E_2, \quad (5)$$

where $m = \rho/\rho_0 - 1$ is the relative compression, ρ/ρ_0 is the ratio of the current density to the initial density, E_2 is the internal energy per unit volume and C_0 through C_6 are the polynomial coefficients.

For ideal gas modelling, the coefficients are simplified to: $C_0 = C_1 = C_2 = C_3 = C_6 = 0$, and $C_4 = C_5 = \gamma - 1$, where γ is the adiabatic exponent. Substituting these values reduces the equation of state to the classical ideal gas form:

$$p = (\gamma - 1)\frac{\rho}{\rho_0} E_2. \quad (6)$$

In this study, the dynamic viscosity of air was set to zero ($\mu = 0$). This is justified because its influence on the pressure exerted on the deminer's external surfaces at a close range to the explosion source is considered negligible. Moreover, including air viscosity would significantly increase the computational complexity of the model without yielding substantial benefits in accuracy for this scenario.

The specific parameters defining the air properties used in the simulations are summarized in Table 4.

Table 4. Parameters of air

Density, kg/m^3	Dynamic viscosity, Pa·s	γ	C_0	C_1	C_2	C_3	C_4	C_5	C_6	E_2, MPa
1.2255	0	1.4	0	0	0	0	0.4	0.4	0	0.2533

3.4 Ground Modelling

Under explosive loading, ground deformation is not limited to deviatoric mechanisms; the behaviour of porous materials is governed by complex three-phase compressibility, particularly in saturated and partially saturated states. Accurate numerical modelling requires considering the compressibility of both the mineral matrix and the pore-filling constituents, including water and air.

Several studies, including references [3] and [18], highlight that the Pressure-Dependent Yield Model (Mode I), based on the Mohr-Coulomb yield surface with a Tresca tensile limit and an appropriate compaction equation of state, is an effective approach for simulating soil response to explosive actions. This model accounts for the dependence of yield strength on mean stress (pressure) and explicitly incorporates volumetric deformation, which is a crucial failure mechanism in porous structures under dynamic loading. Overall, it strikes a good balance between numerical stability, physical accuracy, and predictive performance for blast simulations in ground media.

In LS-DYNA, this model is implemented through two keyword cards [3, 13, 18]:

*MAT_PSEUDO_TENSOR (MAT_016), which governs the mechanical (shear strength) behaviour of the soil.

*EOS_TABULATED_COMPACTION (Form 8), which defines the volumetric response of the material.

The *MAT_PSEUDO_TENSOR card enables the specification of Mode I, which corresponds to the Mohr-Coulomb failure surface with a tensile cutoff based on the Tresca criterion [13]. The shear failure envelope is described by the relationship between the principal stresses difference $(\sigma_1 - \sigma_3)/2$ and the mean pressure *p*. To define this failure envelope, the following input parameters are required: mass density, shear modulus, and tensile cutoff stress.

The *EOS_TABULATED_COMPACTION card defines the equation of state using tabulated pressure vs. volumetric strain data and a bulk unloading modulus [13]. This separation between mechanical strength and volumetric thermodynamics allows for a realistic simulation of soil behaviour over a broad range of pressures, including both compaction and decompaction regimes.

In this study, the influence of ground reflections and the realistic mechanical properties of soil on the stress-strain response of the gas-detonation deminer structure were evaluated. Since the properties of soil media vary significantly depending on their composition, moisture content, and density, four representative sandy soils were selected for numerical modelling: Unwashed Sand (Unw), Low-Density Dry Sand (LDD), High-Density In-Situ Moisture Sand (HDI), High-Density Flooded Sand (HDF).

All necessary physical and mechanical properties for defining the *MAT_PSEUDO_TENSOR and *EOS_TABULATED_COMPACTION cards were obtained from [19]. For each soil type, the required input parameters were specified, including mass density, shear modulus, unloading compressive modulus, pressure cut-off, and the tabulated data for compaction behaviour.

Figure 2(a) presents the shear strength envelopes, expressed as the relationship between the principal stress difference and mean pressure, used to construct the yield surface. Figure 2(b) shows the pressure vs. volumetric strain (*p* vs. ε_V) curves that describe the compressive behaviour of each material and are used in the equation of state. The numerical values for all other input parameters are summarized in Table 5.

Table 5. Additional physical and mechanical parameters of soils

Soil type	Properties			
	Density, kg/m³	Shear modulus, MPa	Bulk unloading modulus, MPa	Pressure cutoff, kPa
HDI Sand	1603	3.254	110.9	0
LDD Sand	1282	1.386	224.0	0
HDF Sand	1443	3.620	131.5	0
Unw Sand	2095	2.303	133.6	-6.895

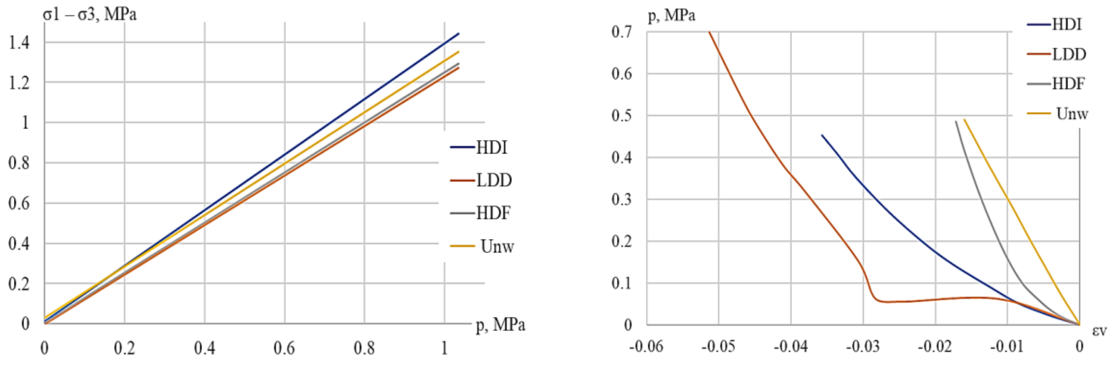

Figure 2: Physical and mechanical characteristics of soil:
a) Strength envelopes of different sandy soils; b) Equation of State curves of different sandy soils.

4. Results of Numerical Experiments

4.1 Validation of the Mathematical Model

Validation of the numerical model was carried out by analysing the sensitivity of the results to the number of active degrees of freedom, with a particular focus on the resolution of the finite element mesh.

A series of simulations were performed to determine the optimal mesh discretization parameters for both the Lagrangian bodies and Eulerian domains.

For the Lagrangian domain, accuracy was assessed using a "mine-air-deminer" model by studying the convergence of the kinetic energy absorbed by the deminer structure in response to the blast wave. Additionally, the amplitude of displacements at the flange of the gas supply pipe closure identified as the most ductile element in bending was analysed as a control parameter. Figure 3 and Figure 4 illustrate how these metrics converge as the number of finite elements increases, with corresponding average element sizes indicated.

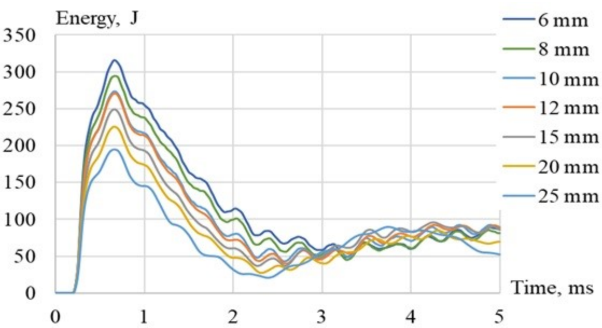

Figure 3: Dependence of the kinetic energy perceived by the deminer in the mine-air-deminer model on the grid parameters in explosion simulations

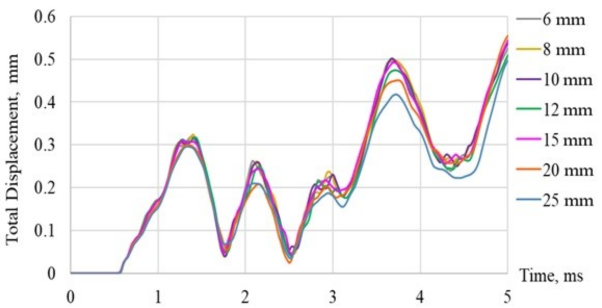

Figure 4: Convergence of maximum amplitude displacements of the gas supply pipe end flange as a function of the number of finite elements

Analysis of the results (Figure 3 and Figure 4) shows that an average finite element size of 10 mm achieves convergence in key metrics namely, the kinetic energy and the flange displacement amplitude. The values obtained for 10 mm and 12 mm are nearly identical, indicating the solution's stability and consistency. In contrast, finer discretization (6 mm and 8 mm) exhibits increased graph waviness and local oscillations. This behaviour likely results from the accumulation of numerical errors, which is typical in explicit integration schemes under high stress gradients and short-duration impulse loading. Although the displacement amplitude varies only slightly across models with element sizes from 15 mm to 6 mm, the 10 mm mesh demonstrates the most stable behaviour with a favourable balance between accuracy and computational cost. There-fore, a 10 mm element size was adopted for all Lagrangian components in subsequent simulations.

For Eulerian domains, mesh resolution was evaluated using a "mine-air-soil" model. Wave reflection from the deminer structure was neglected due to its minimal effect on the results. The soil type used was HDI SAND (see Table 5).

The optimal Eulerian mesh was determined based on a convergence analysis of crater geometry at 2 ms after detonation. Measurements were taken along the crater contour in a central plane intersecting the axis of the deminer pipe. Eulerian element sizes ranged from 100 mm to 20 mm. The results are shown in Figure 5.

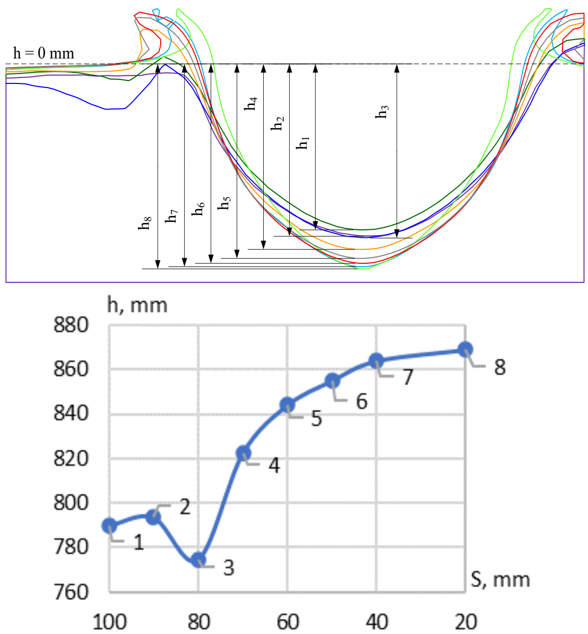

Figure 5: Investigation of the convergence of crater geometry depending on the size of Eulerian elements (S) at time 2 ms: a) convergence of the crater shape in the central section, b) convergence of the maximum crater depth (h)

Figure 5 shows that as the Eulerian element size decreases, the crater shape stabilizes into a more defined elliptical form, with clearer boundaries for the soil ejection zones. Using crater depth as the primary convergence criterion, stabilization is achieved at an element size of 40 mm, resulting in a calculation error of 1.6%. However, following the recommendations in [2], it is important that the Lagrangian and Eulerian mesh sizes remain comparable. To ensure both accuracy and compatibility in the coupled Arbitrary Lagrangian-Eulerian formulation, this study employs average element sizes of 20 mm for the Eulerian domains, which yield a calculation error of 0.6%, and 10 mm for the Lagrangian bodies (see Figure 1).

4.2 Influence of Soil Domain Size on Crater Shape and Dimensions

While the geometric parameters of most model components are well-defined, the greatest uncertainty in the simulation setup relates to the definition of the soil computational domain. Determining the appropriate dimensions of this domain is crucial to accurately capture its stiffness and damping behaviour and to mitigate boundary effects. This is particularly important when modelling explosive loading, where soil is not only compressed but also displaced and ejected, potentially striking structural components.

Among the geometric parameters of the ground domain, its vertical extent (depth) exerts the greatest influence. In contrast, the horizontal dimensions are primarily governed by the relative positions of the mine, the deminer, and the expected extent of soil deformation, including the final crater diameter. In this study, HDI SAND was selected as the representative soil type (see Table 5), under the assumption that small deviations in material properties would not significantly affect the overall crater morphology.

A series of numerical experiments were conducted with the vertical dimension of the soil domain (H) varying from 900 mm to 2000 mm. The results are presented in Figure 6, which illustrates the convergence of the maximum crater depth at 20 ms as a function of H. This time frame corresponds to the moment when the crater reaches its maximum theoretical diameter of D = 1.6 m [20].

The formation of the crater contour (see Figure 6) from a mine detonation on the ground surface is directly influenced by the initial height of the computational ground domain. Results indicate that the shape and depth of the crater stabilize once the soil domain reaches a height of 1500 mm. Beyond this height, further increases have a negligible effect on the crater profile.

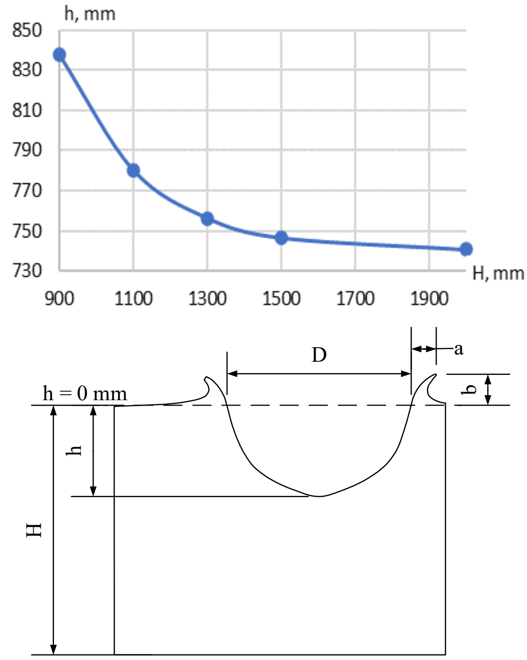

Figure 6: Convergence of crater depth as a function of calculated soil domain size

At a height of 1500 mm, the topsoil lift ("b") and the radial displacement towards the deminer ("a") measured 265 mm and 250 mm, respectively (refer to Figure 6). Fine soil particles were dispersed up to approximately 440 mm in height and 570 mm laterally, while the external structural elements of the deminer (the plate and support struts, as shown in Figure 1) remained unaffected.

Consequently, all subsequent simulations in this study use a soil domain height of 1500 mm. This value provides sufficient modelling accuracy (error below 1%) without unnecessarily enlarging the computational domain.

4.3 Justification of the Ground Model Choice for Evaluating the Effects of Direct and Reflected Blast Waves on the Deminer Structure

In the numerical simulation of detonation wave propagation and its impact on the deminer structure, two fundamentally different approaches were considered for modelling the ground-air interface. In the first approach, the ground surface is idealized as a boundary condition without a geometric soil domain. It is modelled either as a slip boundary (Slip BC), which prohibits flow in the normal direction, or as a free surface (Free BC), which allows wave transmission without reflection.

In the second approach, the soil is explicitly included in the model as a separate physical domain (see Figure 1), with realistic physical and mechanical properties obtained from experimental data (Table 5, Figure 2).

The objective of this study is to assess the influence of these different modelling approaches on the predicted response of the structure and to quantify the discrepancies between the simplified and more physically accurate ground modelling methods.

Specifically, we examine how soil properties and ground reflection affect the development of the dynamic response.

Figure 7 and Figure 8 present the key results for the time (τ) interval from 0 to 10 ms, during which the primary and reflected blast waves produce their peak effects on the structure. Figure 7 illustrates the time history of the structure's kinetic energy (a) and internal energy (b), while Figure 8 shows the total displacements (TD) of the protective plates (a) and the evolution of equivalent von Mises stresses (ES) in the frame struts of the protective casing (b).

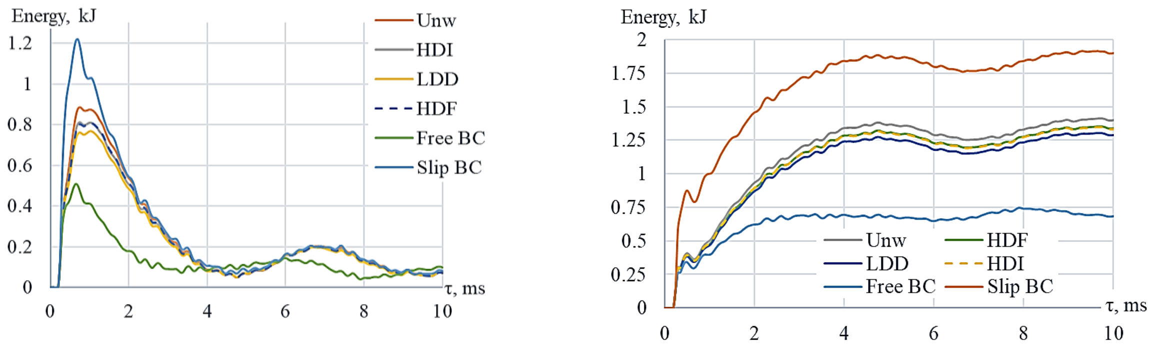

a) b)

Figure 7: Kinetic (a) and internal (b) energies of the deminer at different ground models

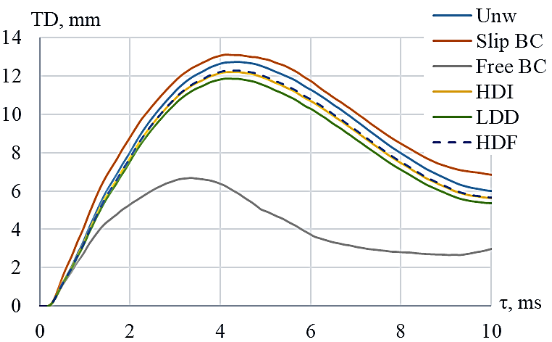

a)

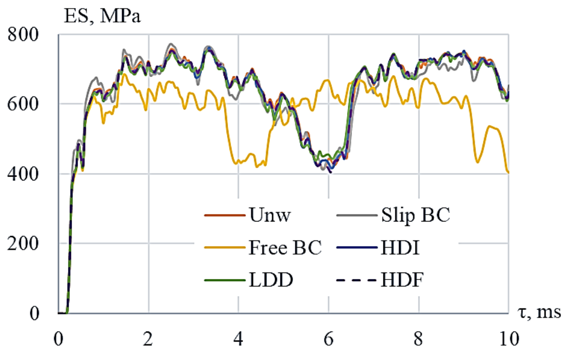

b)

Figure 8: Variation of the total displacements of the containment plates (a) and equivalent Mises stresses in the frame struts of the containment shell (b) over the design time interval.

Analysis of the kinetic energy plots (Figure 7a) reveals a well-defined first peak in all models, corresponding to the initial frontal impact of the shock wave on the deminer structure. This peak occurs between 0.1 ms and 2 ms, and its timing and amplitude are largely unaffected by variations in soil type. However, they are significantly influenced by whether the ground is included as a physical component in the model. The impact of reflected shock waves becomes evident in the later stages of the simulation, specifically between approximately 6 ms and 9 ms. It is important to note that the effect of the reflected wave on kinetic energy is less pronounced than its effect on internal energy (Figure 7b), where it significantly contributes to structural deformation. In fact, the levels of internal energy generated by reflected waves often approach those produced by the initial impact, indicating a prolonged and severe structural response.

These findings highlight the critical importance of including the ground as a physical domain to realistically capture the energy transfer and deformation processes involved. When comparing realistic ALE-based ground models with idealized boundary condition approaches, substantial discrepancies emerge: peak kinetic energy values (Figure 7a) differ by 30–40%, while internal energy values (Figure 7b) differ by 25–45%. In contrast, variations in the physical and mechanical properties of different soils produce only minor differences in energy metrics, on average no more than 15%.

The graphs in Figure 8 further emphasize the importance of accurately representing the ground when modelling explosive impacts on nearby structures. A comparison between models that include the ground as a physical domain and those that use idealized boundary conditions shows that the latter can result in significant distortions in the predicted stress-strain state of the structure. When the wave is either not reflected from the ground surface or does not propagate back to the structure, the models significantly underestimate both the maximum total displacements and peak stresses. Consequently, these simplifications fail to capture the complete destructive potential of the blast. In contrast, employing "hard reflection" conditions allows for a greater transfer of energy to the structure, potentially leading to an overestimation of the initial momentum. While this approach does not fully represent the actual interaction between blast waves and deformable soil (which absorbs some energy and influences the nature of the reflection), it is more suitable for simplified modelling without including a physical soil domain. This method provides a conservative estimate that ensures a safety margin for the structure.

5. Conclusions

Optimal discretization sizes for the computational domains were determined by analysing the convergence of the kinetic energy and maximum displacement amplitudes of the deminer structure. This process balanced accuracy with computational efficiency, ensuring the minimization of resource costs.

The optimal size of the soil computational domain was determined by investigating the convergence of the crater shape. This is a critical factor for accurately modelling the formation and propagation of the secondary shock wave as it impacts the deminer structure.

The shock wave reflected from the ground contributes to the accumulation of in-ternal energy and the stress-strain state of the structure to a degree comparable to the primary wave from the mine detonation. It was established that to accurately reproduce the deminer's dynamic behaviour, it is essential to use models that incorporate the actual mechanical properties of the soil. While all four types of sandy soils (Unwashed Sand, LDD, HDI, HDF) yielded qualitatively similar results, they showed significant quantitative differences. The use of simplified boundary conditions, such as a free surface or a slip-reflecting wall, led to substantial errors in determining the stress-strain state of the structure.

In situations where reliable soil property data is unavailable, it is advisable to use a "mine-air-structure" model with a slip boundary condition at the soil-air interface. This approach provides a conservative upper bound for the structural strength of the device by ensuring maximum load estimations.

The developed hybrid numerical model (ALE-model) effectively reproduces the key mechanisms of medium-structure interaction, including crater formation, ground detachment, and wave reflection from the surface. This model provides an adequate transfer of impulse loads and enables a reliable prediction of the device's behaviour under various geotechnical conditions. The results obtained from this model will be used to optimize the deminer's design.

Acknowledgments

The authors are expressing their gratitude to CADFEM UA LLC, the Channel Partner of Ansys Inc. in Ukraine, for help with the software licensing.

References

[1] Pavlenko, O., Shypul, O., Myntiuk, V., Tkachenko, D., Brega D., Garin V. Development of a conceptual model for a gas detonation deminer. Aerospace technic and technology. 2024, 6 (200), 70-79. DOI:10.32620/aktt.2024.6.07
[2] LS-DYNA Homepage, https://lsdyna.ansys.com, last accessed August 1, 2025.
[3] Barsotti M., Sammarco E., Stevens D. Comparison of Strategies for Landmine Modeling in LS-DYNA with Sandy Soil Material Model Development. 11th European LS-DYNA Conference. Detroit, USA, June 12-14, 2016.
[4] Schwer L., Teng H., Souli M. LS-DYNA Air Blast Techniques: Comparisons with Experiments for Close-in Charges. 10" European LS-DYNA Conference 2015, Würzburg, Germany, 2015.
[5] Trajkovski J. Comparison of MM-ALE and SPH methods for modelling blast wave reflections of flat and shaped surfaces. 11th European LS-DYNA Conference. Salzburg, Austria, 2017.
[6] Gong C., Qiu Y., Long Z., Liu L., Xu G, Yang L. Study on the Earth-Covered Magazine Models under the Internal Explo-sion. Shock and Vibration. 2024, Volume 2024, 20. https://doi.org/10.1155/2024/6626486
[7] Lee S., Lee H., Lee J., Kim Y., Choi G. Shock Response Analysis of Blast Hardened Bulkhead in Naval Ship under Internal Blast. 10th European LS-DYNA Conference 2015, Würzburg, Germany, 2015.
[8] Castedo R., Natale M., López L.M., Sanchidrián J.A., Santos A.P., Navarro J., Segarra P. Estimation of Jones-Wilkins-Lee parameters of emulsion explosives using cylinder tests and their numerical validation. International Journal of Rock Mechanics and Mining Sciences. December

2018, Volume 112, 290-301. https://doi.org/10.1016/j.ijrmms.2018.10.027

[9] Teng H., Wang J. Particle Blast Method (PBM) for the Simulation of Blast Loading. 13th International LS-DYNA Users Conference 2014. Detroit, USA, 2014.

[10] Borvik T., Olovsson L., Hanssen A.G., Dharmasena K.P., Hansson H., Wadley H.N.G. A discrete particle approach to simulate the combined effect of blast and sand impact loading of steel plates. Journal of the Mechanics and Physics of Solids. May 2011, Volume 59, Issue 5, 940-958. https://doi.org/10.1016/j.jmps.2011.03.004

[11] LS-DYNA Keyword User's Manual, Volume I (2025).

[12] Myntiuk, V., Tkachenko, D., Pavlenko, O., Shypul, O. Simulating the Effect of Mine Explosion on a Remote Gas Detonation Deminer. Integrated Computer Technologies in Mechanical Engineering - 2024. ICTM 2024. Lecture Notes in Networks and Systems. 2024, vol 1474. Springer, Cham. https://doi.org/10.1007/978-3-031-94852-7_37

[13] LS-DYNA Keyword User's Manual, Volume II, Material Models, (2025).

[14] Cowper G.R., Symonds P.S., Strain hardening and strain rate effect in the impact loading of cantilever beams, Applied Mathematics Report, 1958., Brown University, 28.

[15] Lee E., Finger M., Collins W., JWL equation of state coefficients for high explosives, Lawrence Livermore Laboratory, University of California/Livermore, California, 1973.

[16] Dobratz B.M., LLNL Explosives Handbook Properties of Chemical Explosives and Explosive Simulants, Livermore, CA, UCRL-51319: Lawrence, Livermore National Laboratory, 1981.

[17] Hamiltom J., Coleman D., Effect of Explosive Charge Geometry on Boundary Surface Peak Pressure with Regard to Standoff Distance. 15th International LS-DYNA Conference. Detroit, USA, 2018.

[18] Courtney L. B. Understanding the Behavior of Embankment Dams Under Blast Loading. Doctor of Philosophy. The Uni-versity of New Mexico Albuquerque, New Mexico, November 2016.

[19] Thomas M. A., Chitty D. E., Gildea M. L., T'Kindt M. C. NASA/CR-2008-215334.Constitutive Soil Properties for Un-washed Sand and Kennedy Space Center. National Aeronautics and Space Administration Langley Research Center, Hampton, Virginia, 2008.

[20] Xu R., Chen L., Zheng Y., Li Z., Cao M., Fang Q. Study of Crater in the Gobi Desert Induced by Ground Explosion of Large Amounts of TNT Explosive up to 10 Tons. Shock and Vibration. 2021, Volume 2021, 17. https://doi.org/10.1155/2021/7357877.